JACS
JOURNAL OF THE AMERICAN CHEMICAL SOCIETY

COMMUNICATION

pubs.acs.org/JACS

Capture of Volatile Iodine, a Gaseous Fission Product, by Zeolitic Imidazolate Framework-8

Dorina F. Sava,[†] Mark A. Rodriguez,[‡] Karena W. Chapman,[⊥] Peter J. Chupas,[⊥] Jeffery A. Greathouse,[§] Paul S. Crozier,[∥] and Tina M. Nenoff*[,†]

[†]Surface and Interface Sciences Department, [‡]Materials Characterization Department, [§]Geochemistry Department, and [∥]Scalable Algorithms Department, Sandia National Laboratories, Albuquerque, New Mexico 87185, United States

[⊥]X-ray Science Division, Advanced Photon Source, Argonne National Laboratory, Argonne, Illinois 60439, United States

Supporting Information

ABSTRACT: Here we present detailed structural evidence of captured molecular iodine (I_2), a volatile gaseous fission product, within the metal−organic framework ZIF-8 [zeolitic imidazolate framework-8 or Zn(2-methylimidazolate)$_2$]. There is worldwide interest in the effective capture and storage of radioiodine, as it is both produced from nuclear fuel reprocessing and also commonly released in nuclear reactor accidents. Insights from multiple complementary experimental and computational probes were combined to locate I_2 molecules crystallographically inside the sodalite cages of ZIF-8 and to understand the capture of I_2 via bonding with the framework. These structural tools included high-resolution synchrotron powder X-ray diffraction, pair distribution function analysis, and molecular modeling simulations. Additional tests indicated that extruded ZIF-8 pellets perform on par with ZIF-8 powder and are industrially suitable for I_2 capture.

Concerns with increased worldwide energy demands, balanced with the need to reduce greenhouse gas emissions, have fueled research on clean, safe, and responsible nuclear energy.[1] A main issue of concern for safety associated with nuclear energy is appropriate nuclear waste management.[2] Concerted efforts have been directed toward optimizing separation processes for complex nuclear waste streams and designing appropriate waste forms.[3] Main components of such waste streams include ^{99}Tc, ^{137}Cs, and ^{90}Sr fission products, minor actinides, lanthanides, and volatile radionuclides. Particularly challenging is the capture of volatile gaseous fission products from nuclear fuel reprocessing or inadvertent environmental release. These radionuclides include ^{129}I and ^{131}I, ^{3}H, $^{14}CO_2$, and ^{85}Kr. Of these, radiological iodine poses exceptional issues. Iodine (I_2) is a highly mobile gas whose individual isotopes present unique exposure problems: ^{129}I is a particularly long-lived isotope (half-life of 1.57×10^7 years) that must be captured and reliably stored while it decays, whereas the ^{131}I isotope is short-lived (half-life of 8.02 days) but requires immediate capture because it directly affects human metabolic processes.[4] Current methods[5a] to capture I_2 by porous adsorbents include the use of silver-exchanged zeolites.[5b] These materials are robust but lack high adsorption capacities because of their limited available surface areas. Further concerns related to cost and environmental impact are also associated with the use of silver metal. Subsequent storage of radioactive iodine in a durable waste form is required, and several methodologies are being pursued, including wet scrubbing,[6] crystallization in mineral analogues[7] and encapsulation in low-temperature sintering glasses.[8]

Here we report a detailed investigation that for the first time demonstrates the efficacy of using metal−organic frameworks (MOFs) as high-capacity iodine adsorbents. This approach allows for secure isolation and concentration of I_2 gas, which then can be easily incorporated into appropriate waste forms. There have been a few reports of I_2 sorption by MOF systems[9] in which either the uptake was reversible or loss of I_2 occurred at moderate temperatures. Our study focuses on the structure−property relationship between the adsorbed I_2 and its confinement within the porous host; we demonstrate that cage-trapped I_2 is secured in the pores of ZIF-8 until the framework decomposes at ∼575 K.

ZIF-8[10] was judiciously selected from a broad library of potential MOFs as an ideal trap for molecular I_2 because of its suitable pore aperture size, large specific surface area, and high chemical and thermal stability. ZIF-8 consists of tetrahedrally coordinated Zn atoms linked by 2-methylimidazole (MeIM) ligands; these form a network with an expanded sodalite structure. The β-cages, with diameters of 11.6 Å, are connected via six-membered-ring (6MR) apertures whose diameter of 3.4 Å allows for the directional diffusion of iodine (∼3.35 Å). The smaller four-membered-ring (4MR) windows are too constrained to permit diffusion of any guest molecules. The high symmetry of the ZIF-8 framework and associated pore network can pose particular challenges in locating guests, which are often crystallographically disordered. Thus, a complete understanding of guest binding can be obtained only by combining insights from local and long-range structural probes and molecular simulations.[11] We have utilized complementary studies involving high-resolution synchrotron-based powder X-ray diffraction (PXRD), differential pair distribution function (d-PDF) analysis, and molecular simulations to identify the preferred binding sites for molecular I_2 in ZIF-8 and to gain insight into the structure−property relationship between the occluded gas molecule and the host framework.

Activated samples of crystalline ZIF-8 powder were exposed to I_2 vapor (in what follows, the as-loaded material is denoted as I_2@ZIF-8). Naturally occurring, nonradioactive I_2 was used in all of the experiments. Loadings were conducted under typical fuel reprocessing conditions (350 K and ambient pressure with an

Received: May 24, 2011
Published: July 18, 2011

dx.doi.org/10.1021/ja204757x | J. Am. Chem. Soc. 2011, 133, 12398–12401

Table 1. Sample Loadings of I_2@ZIF-8

	sample 1		sample 2		sample 3	
	bulk	treated	bulk	treated	bulk	treated
wt %	40	30	85	70	125	100
I/Zn	0.7	0.5	1.5	1.3	2.2	1.8
I_2/cage	1.5	1.5	4	4	5.4	5.4

I_2 vapor pressure of 0.014 atm);[12] the maximum adsorption capacity on ZIF-8 was reached relatively quickly (5−12 h), as it is directly proportional to the sample size. This process was undertaken in a hermetically sealed adsorption chamber, and the uptake was determined gravimetrically.

Thermogravimetric analysis−mass spectrometry (TGA−MS) analyses were conducted on bulk samples containing various I_2 loadings (Table 1): (1) 40 wt % I_2 (0.4 g of I_2/g; 0.7 I/Zn); (2) 85 wt % I_2 (0.85 g of I_2/g; 1.5 I/Zn); and (3) 125 wt % I_2 (1.25 g of I_2/g; 2.2 I/Zn). The I_2 loading of 125 wt % is the highest reported value of I_2 uptake by a MOF. Analysis showed similar overall behavior for all of the samples [Figures S2−S5 in the Supporting Information (SI)]. The data indicate that weakly surface-adsorbed I_2 and water were removed by heating the samples at 400 K for 1 h (Figures S6 and S7).

The iodine loading levels after heat treatment (surface desorption) were analyzed and confirmed by inductively coupled plasma mass spectrometry (ICP-MS) to be (1) 30 wt % I_2 (0.3 g of I_2/g; 0.5 I/Zn), (2) 70 wt % I_2 (0.7 g of I_2/g; 1.3 I/Zn), and (3) 100 wt % I_2 (1 g of I_2/g; 1.8 I/Zn). No release of pore-trapped I_2 molecules was evident before collapse of the structure at ~575 K. In what follows, characterization results are identified using the heat-treated I/Zn designations.

The I_2-loaded samples were characterized at 100 K by high-resolution synchrotron-based PXRD at beamline 11-BM at the Advanced Photon Source at Argonne National Laboratory.[13] The PXRD data showed that sample crystallinity was maintained for I_2 loadings up to ~1.3 I/Zn, beyond which the Bragg intensities broadened significantly and were difficult to distinguish from the pronounced diffuse features in the "background". There was a small contraction of the lattice as the I_2 loading increased. Rietveld refinement of a model based on the reported ZIF-8 structure within GSAS[14] provided a reasonable fit to the data. This suggests that the ZIF-8 lattice itself remains relatively unperturbed upon I_2 loading. The residual of the fit showed notable deviations in intensity for the (200) and (310) diffraction peaks; these are associated with increasing occupancy of the pores (Figure 1).

Difference Fourier analysis was used to identify possible I_2 binding sites, and the results suggested that ZIF-8 contains two independent I sites, denoted as I_a and I_b. Each site is crystallographically disordered over six closely located positions that correspond to six overlapping orientations of the I_2 molecule. The crystallographic symmetry generates additional equivalent sites within each pore centered over alternating 6MR rings. This corresponds to 24 overall possible distinct orientations for each I_a and I_b site (Figure 2b). Modeling data were input back into the structural refinements in order to finalize the unit cell loading levels of I_2. Upon comparison with grand-canonical Monte Carlo (GCMC) simulations and careful consideration of all possible orientations at I_a and I_b, it was determined that a maximum of eight I_2 molecules (2.6 I/Zn) could be accommodated inside each cage (Figure 2c and Figure S10) under these conditions. Experimentally,

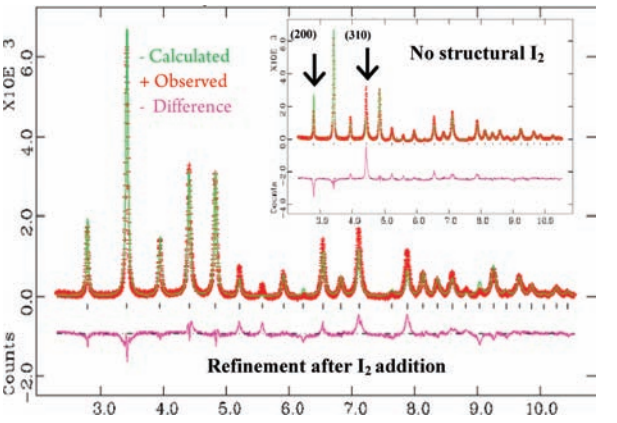

Figure 1. Rietveld structure refinement of I_2@ZIF-8 with I/Zn = 0.5 (inset: refinement fit before I_2 inclusion).

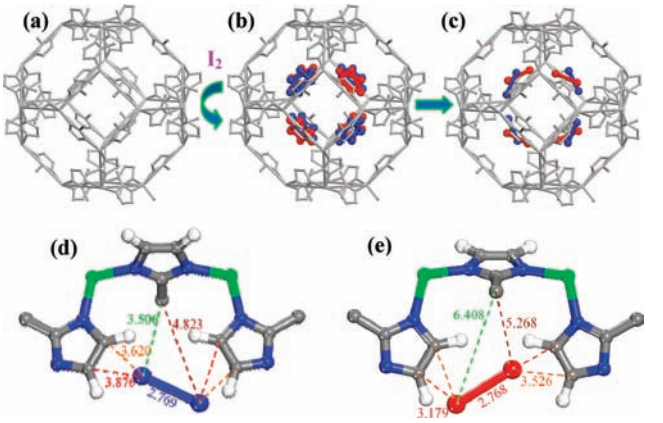

Figure 2. (a) Ball-and-stick model of the activated cage prior to I_2 loading. (b) Two individual molecular I_2 adsorption sites refined inside the β-cage, "I_a" (blue) and "I_b" (red). (c) Actual molecular arrangement (H atoms have been omitted for clarity). (d, e) I_2···framework distances at (d) the I_a site and (e) the I_b site. H atoms of $-CH_3$ groups have been omitted for clarity. Zn, green; C, gray; N, blue; H, white.

we characterized loadings of up to 5.4 I_2 molecules per cage, beyond which the stability of the framework was disrupted.

The PDF method, which provides insight into the local structure as a weighted histogram of the atomic distances independent of sample crystallinity, was implemented to understand the correlated occupancy of the I sites in the crystalline regime (up to 1.3 I/Zn) and beyond (Figure 3a). Total scattering data suitable for PDF analysis were collected using the high-energy X-rays (λ = 0.137024 Å) available at beamline 11-ID-B at the Advanced Photon Source at Argonne National Laboratory. A differential analysis was applied to isolate the contributions involving the I_2 guest molecules (I···I and I···framework correlations) by subtracting a reference PDF measured for the pristine ZIF-8 material, which contained only framework··· framework correlations[15] (Figure 3b). Additional d-PDFs were obtained by progressive subtraction of the PDFs corresponding to intermediate I_2 loadings from those with immediately higher I_2 loadings (Figure 3c). These incremental d-PDFs provide insight into how the different I_2 binding sites become occupied or change with increasing loading (i.e., the adsorption mechanism). Peaks are evident in the d-PDFs at 2.75, 3.23, 4.29, 4.91, 5.46,

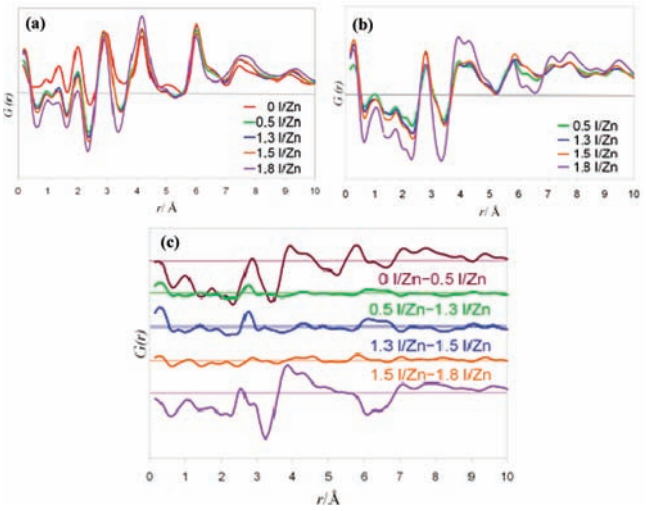

Figure 3. (a) PDFs of I_2@ZIF-8. (b) d-PDFs for various loadings. (c) d-PDFs indicating the I_2 loading mechanism corresponding to the new I···I and I···framework correlations.

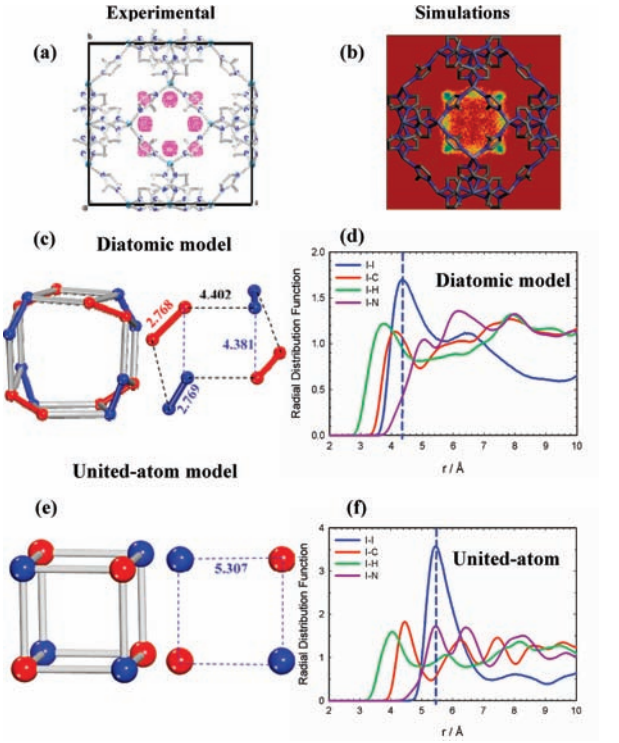

Figure 4. Comparative analyses of experimental and modeling results. (a, b) 2D probability density plots obtained from (a) the experimental difference Fourier map and (b) MD simulations. (c) Distorted octagonal prism formed by refined I_2 molecules. (d) RDF plots generated by MD simulations using the explicit model for I_2. (e) Cubane-like cluster derived from a united-atom model for I_2. (f) Corresponding RDF plots generated by MD simulations using the united-atom model.

6.01, and 6.61 Å upon incremental loading up to the maximum capacity. Because of the strong X-ray scattering of I_2, these features can be attributed to intra- and intermolecular I_2 distances within the ZIF-8 pores. With increased I_2 loading above 1.3 I/Zn, distinct changes in the d-pdfs occur, including new peaks at 2.56, 2.94, and 3.79 Å, increases in the peak intensities at ~4.3 and ~4.9 Å, and decreases in the peak intensity at 3.24 Å, suggesting that a slight rearrangement of the I_2 molecules may be needed to accommodate these additional guests.

Figure 4 depicts the close correlations between the experimental investigations and molecular dynamics (MD) simulations. MD and GCMC simulations were performed using the LAMMPs code[16] with a 2 × 2 × 2 supercell (16 cages) at 298 K. Guest I_2 molecules were modeled using both explicit-atom (diatomic) and united-atom (spherical) approaches.

The time-averaged atomic density plot from the MD simulations (Figure 4b) shows increased density at positions closely related to those indicated in the Bragg analysis. Partitioning between crystallographic I_a and I_b sites cannot be distinguished. The MD simulations capture the dynamic nature of the I_2 molecules. The I_2 molecules are quite mobile within the cage at 298 K even at high loadings, and they freely move between sites within each individual cage. Importantly, the I_2 molecules do not readily diffuse between neighboring cages (see the movie in the SI). The good agreement between the measured PDFs and the radial distribution functions (RDFs) calculated from the simulations validates the insights from modeling. The closest interactions with the framework are I···H and I···C contacts attributable to methyl and methine groups on the imidazole ring. Figure 4c–f highlights this feature in terms of overall intermolecular I_2 interactions.

Furthermore, analysis of the data allowed for the determination of guest-molecule siting and occupancy within the β-cages of ZIF-8 and the effects of I_2 loading on the crystallinity of the framework. The refined bond lengths for both intra- and intermolecular I_2 distances are within the expected ranges and consistent with the PDF data. As such, the I_a–I_a and I_b–I_b distances are 2.7 Å, while the I_a···I_b distances are in the 3.3–4.4 Å range, consistent with expected values.[17] Each refined site is centered over a 6MR window. The closest guest···framework interactions occur between highly polarizable I_2 molecules and the MeIM ligand. This is broadly consistent with other determinations of guest binding sites in ZIF-8,[18] even though a unique guest site was found here. The occupancies of the I_a and I_b sites increased with I_2 loading, although the filling occurred at different rates, with the I_a location maintaining a higher occupancy than I_b. Table 2 summarizes the close contacts between the two refined sites and the framework.

In the pristine material, there are well-defined features in the PDF at long distances, consistent with the long-range crystalline order of the framework. The features at large r progressively broaden with increasing I_2 loading, consistent with a reduction in crystallinity. At the highest loading levels, there are no features in the PDF beyond ~10 Å. However, below ~6 Å, the general features in the PDF are retained at all I_2 loading levels.

These are characteristic of the Zn···MeIM and Zn···Zn′ correlations within the Zn–MeIM–Zn′ linkages, which are retained despite the loss of long-range periodicity. The persistence of the peak at ~6 Å, corresponding to the Zn–(MeIM)–Zn′ distance, indicates that short-range order and the framework connectivity are still maintained. This Zn···Zn′ correlation progressively contracts with increased I_2 loading, possibly because of a distortion of the Zn–MeIM–Zn′ linkages at higher loading levels.[19] This is also evident in the diffraction data for lower I_2 loadings, as indicated by a lattice parameter contraction from 17.029 to 16.933 Å in going from the 0.5 I/Zn to the 1.3 I/Zn composition. Distortion of the Zn–MeIM–Zn′ linkages is unlikely to be correlated between different moieties, so an

dx.doi.org/10.1021/ja204757x |J. Am. Chem. Soc. 2011, 133, 12398–12401

Table 2. Site Occupancy and $I_2\cdots$MeIM Contacts

	site occupancy		contacts with MeIM carbons (Å)	
I site	0.5 I/Zn	1.3 I/Zn	CH_3	HC═CH
I_a	0.28	0.88	3.506, 4.823	3.620, 3.876
I_b	0.14	0.38	5.268, 6.408	3.179, 3.526

uncorrelated distortion of the Zn−MeIM−Zn′ units may underlie the observed loss of long-range translational symmetry (i.e., crystallinity) at high loadings.

To assess the processing applicability of ZIF-8 for volatile I_2 gas capture in nuclear fuel reprocessing or nuclear accident remediation applications, additional tests were conducted on extruded ZIF-8 material.[20] There was no change in the porosity of the sample following the extrusion process, as evidenced by N_2 sorption isotherms (Figure S11); the I_2 sorption behavior of the pellets matched the results for the powdered material. While ZIF-8 represents an excellent high-capacity I_2 adsorbent material, we highlight that it meets the requirement for I_2 capture and only interim storage. Further incorporation into stable waste forms for long-term storage would be needed for final disposal in designated repositories. To address this, we developed a highly flexible, low-temperature method in which the as-loaded I_2@ZIF-8 is encapsulated with minimum additional processing in a durable glass composite material (GCM) waste form. The resulting GCM contains at least 5.5 wt % I_2;[8b] efforts to optimize the composition and loading levels of the GCM are ongoing.

In summary, we have presented a structural study of I_2 capture within ZIF-8 that employed a combination of experiments and molecular simulations. The results suggest that I_2 adsorption is mainly due to favorable interactions with the MeIM linker of the framework. Our findings indicate that up to 5.4 I_2 molecules are captured inside each cage. While increasing distortions of the framework with increased I_2 loadings result in a reduction and eventual loss of the long-range crystalline symmetry, the PDF analyses confirmed that the cage connectivity is retained under these loading conditions, despite the fact that MOF crystallinity has often been used as a measure of framework stability. Most notably, this study acknowledges that ZIF-8 is a highly appropriate capture and interim storage medium for volatile gaseous I_2. Additionally, the material maintains its high adsorption capacity in extruded pellet form (a desired feature, as this is the typical form for porous adsorbents in currently employed separation processes). We anticipate that this study will increase awareness and impact the use of MOFs in the capture of related fission product gases.

■ ASSOCIATED CONTENT

Supporting Information. I_2 loading experiments, TGA−MS analyses, XRD data, PDF analyses, molecular modeling, sample pelletization, and N_2 sorption measurements. This material is available free of charge via the Internet at http://pubs.acs.org.

■ AUTHOR INFORMATION

Corresponding Author
tmnenof@sandia.gov

■ ACKNOWLEDGMENT

This work was supported by the U.S. DOE-NE/FCRD-SWG and -NEAMS. Sandia National Laboratories is a multiprogram laboratory managed and operated by Sandia Corporation, a wholly owned subsidiary of Lockheed Martin Corporation, for the U.S. DOE's NNSA under Contract DE-AC04-94AL85000. Use of the Advanced Photon Source, an Office of Science User Facility operated for the U.S. DOE/Office of Science by Argonne National Laboratory, was supported by the U.S. DOE under Contract DE-AC02-06CH11357.

■ REFERENCES

(1) Kintisch, E. *Science* **2005**, *310*, 1406.
(2) Ewing, R. C.; von Hippel, F. N. *Science* **2009**, *325*, 151.
(3) (a) Weber, W. J.; Navrotsky, A.; Stefanovsky, S.; Vance, E. R.; Vernaz, E. *MRS Bull.* **2009**, *34*, 46. (b) *Waste Forms Technology and Performance: Final Report*; National Academies Press: Washington, DC, 2011.
(4) Lee, W. E.; Ojovan, M. I.; Stennett, M. C.; Hyatt, N. C. *Adv. Appl. Ceram.* **2006**, *105*, 3.
(5) (a) Krumhansl, J. L.; Nenoff, T. M. *Appl. Geochem.* **2011**, *26*, 57. (b) Chapman, K. W.; Chupas, P. J.; Nenoff, T. M. *J. Am. Chem. Soc.* **2010**, *132*, 8897.
(6) Haefner, D. R.; Tranter, T. J. *Methods of Gas Phase Capture of Iodine from Fuel Reprocessing Off-Gas: A Literature Survey*; INL/EXT-07-12299; Idaho National Laboratory: Idaho Falls, ID, 2007.
(7) Audubert, F.; Carpena, J.; Lacout, J. L.; Tetard, F. *Solid State Ionics* **1997**, *95*, 113.
(8) (a) Garino, T. J.; Nenoff, T. M.; Krumhansl, J. L.; Rademacher, D. X. *J. Am. Ceram. Soc.* [Online early access]. DOI: 10.1111/j.1551-2916.2011.04542.x. Published Online: April 20, 2011. (b) Sava, D. F.; Garino, T. J.; Nenoff, T. M. *Ind. Eng. Chem. Res.* [Online early access]. DOI: 10.1021/ie200248g. Published Online: May 13, 2011.
(9) (a) Lang, J. P.; Xu, Q. T.; Yuan, R. X.; Abrahams, B. F. *Angew. Chem., Int. Ed.* **2004**, *43*, 4741. (b) Wang, Z. M.; Zhang, Y. J.; Liu, T.; Kurmoo, M.; Gao, S. *Adv. Funct. Mater.* **2007**, *17*, 1523. (c) Zeng, M. H.; Wang, Q. X.; Tan, Y. X.; Hu, S.; Zhao, H. X.; Long, L. S.; Kurmoo, M. *J. Am. Chem. Soc.* **2010**, *132*, 2561.
(10) Park, K. S.; Ni, Z.; Côté, A. P.; Choi, J. Y.; Huang, R.; Uribe-Romo, F. J.; Chae, H. K.; O'Keeffe, M.; Yaghi, O. M. *Proc. Natl. Acad. Sci. U.S.A.* **2006**, *103*, 10186.
(11) Vaidhyanathan, R.; Iremonger, S. S.; Shimizu, G. K. H.; Boyd, P. G.; Alavi, S.; Woo, T. K. *Science* **2010**, *330*, 650.
(12) Haefner, D.; Law, J.; Tranter, T. *System Design Description and Requirements for Modeling the Off-Gas Systems for Fuel Recycling Facilities*; INL/EXT-10-18845; Idaho National Laboratory: Idaho Falls, ID, 2010.
(13) Wang, J.; Toby, B. H.; Lee, P. L.; Ribaud, L.; Antao, S. M.; Kurtz, C.; Ramanathan, M.; Von Dreele, R. B.; Beno, M. A. *Rev. Sci. Instrum.* **2008**, *79*, No. 085105.
(14) Larson, A. C.; Von Dreele, R. B. *General Structure Analysis System (GSAS)*; Report LAUR 86-748; Los Alamos National Laboratory: Los Alamos, NM, 2000.
(15) Chapman, K. W.; Chupas, P. J.; Kepert, C. J. *J. Am. Chem. Soc.* **2005**, *127*, 11232.
(16) Plimpton, S. J. *J. Comput. Phys.* **1995**, *117*, 1.
(17) Svensson, P. H.; Kloo, L. *Chem. Rev.* **2003**, *103*, 1649.
(18) (a) Wu, H.; Zhou, W.; Yildirim, T. *J. Am. Chem. Soc.* **2007**, *129*, 5314. (b) Wu, H.; Zhou, W.; Yildirim, T. *J. Phys. Chem. C* **2009**, *113*, 3029.
(19) Wu, Y.; Kobayashi, A.; Halder, G. J.; Peterson, V. K.; Chapman, K. W.; Lock, N.; Southon, P. D.; Kepert, C. J. *Angew. Chem., Int. Ed.* **2008**, *47*, 8929.
(20) For the procedure for binder-free pelletization, see the SI.